Submitted to UGA
7/9/91

GL04720

ANALYSIS OF BEDDING ORIENTATIONS WITHIN A PORTION OF THE FERRON SANDSTONE NEAR EMERY UTAH

Dennis L. Nielson, Susan J. Lutz, Jeffrey B. Hulen
University of Utah Research Institute

Paul B. Anderson
Consulting Geologist

ABSTRACT

The orientations of laminae, bed boundaries and unit boundaries have been measured within three units in the Ferron Sandstone Member of the Mancos Shale in outcrops near Emery, Utah. These measurements simulate the bedding orientation data that would be collected by borehole imaging logs. Data are presented for the #4 and #5 marine sandstones and the system of fluvial and distributary channels that separate the marine units. The data are presented in Statistical Curvature Analysis Technique (SCAT) format. Azimuth data for individual units shows wide distributions that reflect current directions during deposition. Dip angles follow a lognormal distribution with the variance of the distribution correlating with the energy level of the depositional environment.

INTRODUCTION

Improvements in the technology of borehole imaging have resulted in commercial surveys that can collect large amounts of accurate bedding orientation data within wells drilled for oil and gas. The application of borehole imaging logs to the interpretation of depositional environments has a long history in service company publications (Schlumberger, 1986; Atlas Wireline, 1987). Recent advances in imaging and processing techniques have resulted in surveys that can successfully measure dips on foreset beds (Hocker and others, 1990) and give sufficient information to identify sedimentary structures from the imaging logs (Luthi, 1990). We believe that these data can be analyzed statistically to characterize sedimentary facies and to predict the threedimensional architecture of those facies. In order to test and refine these concepts, the Cretaceous Ferron Sandstone Member of the Mancos Shale in Emery County, Utah has been used as an analog for hydrocarbon reservoir rocks deposited in fluvial-deltaic environments.

Simulation of data from borehole imaging logs has been accomplished by measuring a series of vertical sections through outcrops of different units of the Ferron Sandstone. These measurements, obtained using a Brunton compass, have documented dip angles and azimuths of sedimentary features through the sections.

The data have been analyzed using a statistical curvature analysis technique (SCAT; Bengtson and Ziagos, 1987; Nielson and others, 1991) that has been used previously in the analysis of structural features from borehole imaging logs (Bengtson, 1981). SCAT plots differ from standard dip arrow representations in common use by logging companies. The SCAT approach resolves the data into components of dip and azimuth that are separately plotted as a function of depth. The method also calculates the components of dip in the longitudinal and transverse directions. The transverse direction is defined as the direction with the maximum number of dip orientations while the longitudinal direction is at right angles to the transverse. The bulk curvature of stratigraphic bodies or structural features is evaluated by making polar tangent plots (Bengtson, 1980) or cross plots of dip vs. azimuth (DVA) data. In this paper, we will be using plots of dip and azimuth components as a function of depth and DVA plots.

Our work (Nielson and others, 1991) has shown that plots of dip and azimuth as a function of depth are effective at distinguishing different sedimentary units within a stratigraphic sequence. In addition, this work has shown that many sedimentary structures have geometries, or bulk curvatures, similar to those of folded rocks (see also Perrin, 1975). However, it is also clear that many sedimentary features have no similarity with geometries exhibited by folded rocks. We will see some examples of each in this paper. The application of statistics could be of use in defining sedimentary processes and the paleo-environmental implications of bedding orientation data, and we begin to develop some of that information in this paper.

GEOLOGIC RELATIONSHIPS

The Ferron Sandstone Member of the Mancos Shale is a well-exposed example of rocks deposited in a fluvial-dominated deltaic system. The outcrop pattern of the Ferron along the flanks of the San Rafael Swell, is shown in Figure 1. The Ferron has been described by Ryer (1981a), and the reader is directed to that publication for more complete descriptions of the stratigraphic units. The depositional environment of the Ferron Sandstone has been discussed by a number of authors, and the account of Ryer and McPhillips (1983) summarizes these. Tripp (1989) has compiled well data that complements the study of Ryer and McPhillips. The architecture of the Ferron is the subject of a comprehensive study by Gardner (1991).

Figure 1 shows the locations of stratigraphic sections we have measured in the Ferron to compile data approximately normal to the paleo-shoreline. Figure 2 is redrawn from Ryer (1981b) and shows a stratigraphic cross section approximately normal to the paleo-shoreline. The Tununk Member of the Mancos Formation underlies the Ferron and is composed of off-shore marine shale that thickens to the southwest toward the subsiding foreland basin of the Sevier orogenic belt. The Ferron documents an overall regression of the Cretaceous sea that established shorelines within the prograding delta deposits in the area we are investigating. Ryer (1981a,b) has mapped five major delta front sandstones that represent prograding deltaic units. Vertically and laterally in an updip direction, each of these marine sandstones is overlain by distributary channel and fluvial deposits. Marine transgressions were largely erosional and are poorly preserved. Hale (1972) interpreted the Ferron in this vicinity as a major delta that he named the Last Chance Delta. Ryer and McPhillips, however, concluded the shoreline was characterized by numerous small coalescing deltas. Both Ryer and McPhillips and Hale agree that the southern portion of Castle Valley was the site of a northwest trending shoreline during Ferron time. Ryer (1981a) and Anderson (1991) have mapped the landward pinchouts of the numbers 2 through 5 delta front sandstones, and have found remarkably parallel trends to the northwest.

ORIENTATION DATA

Orientations of laminae, bed boundaries and unit boundaries were measured in a series of vertical sections in the Miller Canyon, Muddy Creek, and Dry Wash areas (Fig. 1). These sites represent a general progression in the ancient delta system from landward in Miller Canyon to seaward at Dry Wash. Dip azimuth and angle of laminae, bed boundaries, and unit boundaries were recorded and tied to detailed stratigraphic sections at intervals of one foot or less. For the sections presented in this paper, measurements of these different orders of features have been combined. Tests have shown that there is little difference between the orientations of these different orders of bounding surfaces for the units discussed in this paper. However, this is not always the case.

All orientation data from the measured sections contained a component of regional dip resulting from uplift along the flank of the San Rafael Swell (Fig. 1). Note that this regional dip facilitates the accurate measurement of flat dips that would otherwise be associated with measurement error and increased data scatter. The data presented here have had the regional structural dip removed in order to more accurately represent original sedimentary orientations. The regional dip was determined using the orientations of bedding surfaces that can be assumed to have been deposited in a horizontal attitude. The following regional dips have been removed from the sections: Muddy Creek sections, N30E, 7NW; Miller Canyon sections, N10E, 9W; Dry Wash sections, N10E, 10W.

This paper will concentrate on the relationships of the #4 and #5 marine sandstones and the system of fluvial and distributary channels that lies between these two marine units (Fig. 2).

#4 Marine Sandstone

The #4 marine sandstone of Ryer (1981) was deposited by a prograding delta front. Although the landward pinchout of this unit has been obscured by erosion, Ryer (1981) has been able to trace its location in the subsurface using well information. The approximate location and trend of this pinchout, which shows the trend of the shoreline at the time of the maximum transgression prior to the deposition of the #4, is shown in Figure 1.

Outcrop dip data from the #4 marine sandstone is available from the three areas in which measurements were made. The Miller Canyon sections are closest to the landward pinchout of the unit. Here the sandstone has been extensively bioturbated, and original sedimentary laminations are not preserved. Sedimentary structures that are present consist of planar bedding, hummocky and low-angle cross bedding and ripple laminations.

In the Muddy Creek area, the rocks are principally ripple laminated and hummocky cross stratified. Low-angle and trough cross beds also make up part of the unit, and bioturbation is minor.

In the distal Dry Wash sections, the unit is all marine and the sandstones are interbedded with shales. Hummocky cross stratification is the principal sedimentary structure found in these rocks.

Figure 3a is a plot of dip vs azimuth (DVA) for all the orientation data collected from the #4 marine sandstone. This type of plot is made to document the bulk curvature of the sandstone body (Bengtson, 1981; Bengtson and Ziagos, 1987; Nielson and others, 1991). The data shows a bimodal distribution that becomes even more apparent when a histogram is created for the azimuth data (Fig. 3b). The principal concentration of these points is at an orientation of -35 degrees. The secondary peak occurs at about 130 degrees, representing an angular separation of the peaks of about 165 degrees. Both concentrations of azimuth data appear to have a normal distribution.

Figure 4 shows dip and azimuth plots as a function of depth for a series of measured sections of the #4 Sandstone. In the azimuth plots for the Dry Wash sections, the character of the bimodal distribution becomes apparent. In both the DW-4 and 6 sections, the southeastern azimuths occur scattered within sections that predominantly dip to the northwest. In the DW-5 section, however, the lower portion of the section, representing distal bar facies (lower shoreface) dips to the northwest. The upper portion of the section is a distributary mouth bar and dips are preferentially oriented toward the southeast.

These measurements show that the principal direction of sediment transport was to the northwest, nearly parallel to the trend of the shoreline as defined by Ryer's pinchouts. There are two possible explanations for this. The first is that since the pinchouts represent the point of maximum transgression of the sea, the depositional environment may have changed by the time the sandstones we measured were deposited. This explanation is unlikely for two reasons. First, all sections measured contain the northwest trend, not just those in the most distal parts of the environment. Second, the pinchouts mapped by Ryer (1981a) and confirmed by Anderson (1991) are remarkably parallel and suggest a paleo-shoreline that was consistent through time.

The more plausible explanation is that the sections were measured on the northwest portion of a delta prograding to the northeast. We believe the bedding orientations, along with the paleo-shoreline trend, indicate that the sections measured are to the left (facing downstream) of the depositional axis of the delta.

Selley (1989) has proposed using dipmeter logs to document the rotation of azimuths through a deltaic unit, and, from this, infer the position of a well with respect to the axis of the delta. In the Dry Wash area, sections 4,5, and 6 are sufficiently separated from one another that Selley's hypothesis can be tested. Figure 4 shows dip azimuth diagrams for these sections. Sections DW-4 and the lower portion of DW-5 show an apparent counterclockwise rotation of dip moving up section. By Selley's model, this would indicate that these two sections are located on the left side of the depositional system (facing down stream). Section DW-6 shows no rotation suggesting it is located along the axis of the prograding delta. The data are consistent with the locations of these sections.

In contrast with the azimuth distribution, a histogram of dip data from the #4 marine sandstone shows a lognormal distribution (Fig. 3c). The range of dips has often been cited as being related to the energy of the depositing system (Bengtson and Ziagos, 1987; Atlas Wireline, 1987) or to the depth of water during deposition (Schlumberger, 1986). These generalizations are correct, but our studies in the Ferron have suggested that the mean and variance of dip data can greatly contribute to the identification of sedimentary facies.

The lognormal distribution is a skewed distribution that is not especially easy to characterize statistically. We have calculated the median

$$\gamma = e^{\alpha}$$

where α is the average of the logarithms. Also shown (Fig. 3c) are the unbiased efficient estimate of the mean (m) and unbiased efficient estimate of the variance (V^2) calculated by the methods described in Koch and Link (1971, p. 218). An unbiased estimate refers to the property that the sample parameter is equal to the population parameter. An efficient statistic is one with the smallest mean square error of any that might be calculated. The standard deviation (V) is the square root of the variance.

Channels Between #4 and #5 Marine Sandstones

The prograding system that deposited the #4 marine sandstone resulted in a vertical succession to distributary channels followed by delta plain deposits. The channel facies are present in sections measured at Miller Canyon and Muddy Creek.

An excellent exposure of a fluvial channel in Miller Canyon can be used to show the similarity between the bulk curvature of a filled channel and that of folded strata. Figure 5a shows an interpreted cross-section of the channel and the areas where two sections were measured. Figure 5b shows the DVA plot containing the data from both the ML-1 and 2 sections (Note that this particular plot does not have the regional dip removed). ML-1 is largely composed of accreting point bar sands that dip to the northwest. The ML-2 section is located within the main part of the channel and has dips at varying angles to the northeast. The pattern developed here is similar to that which would be expected from a conical or plunging fold (Bengtson, 1981). This type of analysis makes determination of the depositional axis of the sandstone body clear; it is the point at the center of the horseshoe.

Figure 6a is a DVA plot of all the measurements (both Miller Canyon and Muddy Creek) from the channel system located above the #4 marine sandstone. A pattern of bulk curvature that is analogous to patterns seen for folded rocks is difficult to see from this plot. The histogram of dip azimuths (Fig. 6b) is different than those for the #4 sandstone. The distribution is much broader and is probably a composite of a number of populations. However, the dip azimuth maximum of -55 degrees is very close to the direction of maximum transport for the underlying #4.

The histogram of dips (Fig. 6c) contains two separate lognormal distributions. The population with the steeper dips represents accreting point bar deposits; similar to the data that was shown in Figure 5b.

#5 Marine Sandstone

Above the channel system just discussed, an erosional surface represents a marine transgression or parasequence boundary. The subsequent progradational event is represented chiefly by delta front facies termed the #5 marine sandstone by Ryer (1981a).

The shoreline of the #5 sandstone had approximately the same trend as the #4 (Fig. 1) with the landward pinchout occurring in the Muddy Creek area. Most of our data is from Muddy Creek with the exception of one section from Dry Wash (DW-5).

The DVA for the #5 Sandstone is shown in Figure 7a. There is a much broader distribution of azimuths than was seen in the data for the #4 sandstone. The azimuth histogram (Fig. 7b) shows that these data are also bimodal; but with the concentrations of azimuths oriented 180 degrees apart, to the north and to the south. This suggests a directional change in the locus of sedimentation from the time of deposition of the #4 shoreface and channel sandstones (oriented northwest) to the time of deposition of the #5 sandstone (oriented north-south). The bimodal distribution with concentrations 180 degrees apart suggests the influence of tidal activity within the shoreface sandstones.

The dip histogram for the data again shows a lognormal distribution (Fig. 7c). The distribution of dips in the #5 is not dissimilar from that seen in the #4 (Fig. 3c).

DISCUSSION

Bedding orientation data measured in three units of the Ferron Sandstone have been used to simulate data that would be acquired by borehole imaging logs. The data are analyzed here using a partial Statistical Curvature Analysis Technique (Bengtson and Ziagos, 1987). This technique utilizes the similarity of geometry between sedimentary and fold structures to characterize simple sedimentary features. The channel fill from Miller Canyon (Fig. 5) illustrates this concept and shows the usefulness of DVA plots in determining stream flow directions.

It is apparent from the data collected that the analogy between sedimentary and fold structures is dependent upon the scales of investigation. The analogy holds well for sedimentary structures such as cross bedding (Nielson and others, 1991). However, at the scale of a channel fill, the geometry is dependent upon the mechanism of channel filling. At the scale of the prograding delta-front sandstones, such as seen in the #4 and #5 units in the Ferron, the fold analogy breaks down. However, by breaking dip orientations into their component parts, the SCAT approach provides a mechanism for calculating statistics on the data.

This paper has shown that dip angle and dip azimuth data for the Ferron follow different statistical behaviors. Dip angle data for particular units display a lognormal distribution. Azimuth data appears normally distributed in many instances. Depending on scales of investigation, multiple population can be common.

The central tendency and variance of dip angles is generally related to the energy of the depositional environment. In our analysis of all the data collected in this project (Nielson and others, 1991) it became apparent that the distal delta-front sandstones (excluding mouthbar and tidal deposits) could be identified by their relatively low angle dips and small variance. In the present work we have initiated a data base on these measurements that will be utilized to perform statistical tests for assignment of dips to paleoenvionmental interpretations. The two marine sandstone sections show similar central tendencies of dip angles with medians of 3.7 (#4) and 3.3 (#5). The scatter of the data is different with a variance of 22.2 for #4 and 41.6 for #5. The variance in dip angles is correlated also with the greater scatter in dip azimuths in the #5.

The dip distribution for the #4 marine sandstone is in contrast to that measured for the overlying fluvial channels. Data from the fluvial channels have a median of 6.3, and the scatter is much greater as measured by a variance of 111.6. In addition, this dip angle data is bimodal, reflecting, we believe, the relatively high dips associated with accreting point bar deposits.

The #4 marine sandstone and overlying channel system comprise a parasequence (Van Wagoner and others, 1990). Our analysis of this parasequence demonstrates the overall depositional vector was oriented to the northwest. This remained true even though the depositional environment changed as the delta system prograded. Across the parasequence boundary in the #5 marine sandstone, the depositional vectors have changed.

The data also suggest that the marine deposits in the different parasequences were influenced by different processes as defined in the classification scheme of Galloway (1975). In the #4 parasequence, we suspect that there was a wave or current influence. In the overlying #5 marine sandstone, our data suggests that there is a strong tidal influence.

ACKNOWLEDGEMENTS

This report was compiled from data collected under contract #5089-260-1855 to the University of Utah Research Institute from the Gas Research Institute. This funding is gratefully acknowledged.

REFERENCES

Anderson, P. B., 1991, Potential stratigraphic traps from landward pinch-outs of shoreline facies: examples from east-central Utah: this volume.

Atlas Wireline Services, 1987, Fundamentals of diplog analysis: Houston, Atlas Wireline Services, 216p.

Bengtson, C. A., 1980, Structural uses of tangent diagrams: Geology, v. 8, no. 12, p. 599-602.

Bengtson, C. A., 1981, Statistical curvature analysis techniques for structural interpretation of dipmeter data: American Association of Petroleum Geologists Bulletin, v. 65, p. 312-332.

Bengtson, C. A. and Ziagos, J. P., 1987, Stratigraphic statistical curvature analysis techniques: American Association of Petroleum Geologists Bulletin, v.71, p. 529.

Galloway, W. E., 1975, Process framework for describing the morphologic and stratigraphic evolution of deltaic depositional systems, in Broussard, M. L. (ed), Deltas, Models of Exploration: Houston Geological Society, Houston, p. 87-98.

Gardner, M. H., 1991, Fluvial architecture in the Cretaceous Ferron Sandstone, Utah: Ph.D. dissertation, Colorado School of Mines, in preparation.

Hale, L. A., 1972, Depositional history of the Ferron Formation, central Utah: Utah Geological Association, Publication 2, p. 29-40.

Hocker, C. Eastwood, K. M., Herweijer, J. C. and Adams, T., 1990, Use of dipmeter data in clastic sedimentological studies: American Association Petroleum Geologists Bulletin, v.74, p. 105-118.

Koch, G. S. and Link, R. F., 1971, Statistical analysis of geological data, v.1: New York, Dover, 375p.

Luthi, S. M., 1990, Sedimentary structures of clastic rocks identified from electrical borehole images, in Hurst, A., Lovell, M. A., and Morton (eds), Geological Application of Wireline Logs: Geological Society Special Publication #48, p. 3-10.

Nielson, D. L., Bengtson, C. A., Hulen, J. B., Chan, M. A., Lutz, S. J., Anderson, P. B., Tripp, C. N., and Allison, M. L., 1991, Definition of stratigraphic heterogeneity using borehole imaging: the application of the statistical curvature analysis technique: Gas Research Institute Report GRI-91/0004, 294p.

Perrin, G., 1975, Comparison entre des structures a l'affeurement et les pendagemetries se sondage: Bull. Cent. Resh. Pau-SNPA, v. 9, p. 147-181.
Ryer, T. A., 1981a, Deltaic coals of the Ferron Sandstone Member of the Mancos Shale: predictive model for Cretaceous coal-bearing strata of western interior: American Association of Petroleum Geologists Bulletin, v.65, p.2323-2340.

Ryer, T. A., 1981b, Cross section of the Ferron Sandstone Member of the Mancos Shale in the Emery coal field, Emery and Sevier counties, central Utah: U. S. Geological Survey Misc. Field Studies, Map MF-1357.

Ryer, T. A. and McPhillips, M., 1983, Early Late Cretaceous paleogeography of east-central Utah, in Reynolds, M. W., and Dolly, E. D. (eds), Mesozoic paleogeography of west-central United States: Denver, Rocky Mountain Section, SEPM, p.253-272.

Schlumberger, 1986, Dipmeter interpretation fundamentals: New York, Schlumberger Ltd., 76 p.
Selley, R. C., 1989, Deltaic reservoir prediction from rotational dipmeter patterns, in Whateley, M. K. G. and Pickering, K. T. (eds.) Deltas: sites and traps for fossil fuels: Geological Society Special Publication No. 41, p. 89-95.

Tripp, C. N., 1989, A hydrocarbon exploration model for the Cretaceous Ferron Sandstone Member of the Mancos Shale, and the Dakota Group on the Wasatch Plateau and Castle Valley of east-central Utah, with emphasis on post-1980 subsurface data: Utah Geological and Mineral Survey Open-file Report 160, 81p.

Van Wagoner, J. C., Mitchum, R. M., Campion, K. M. and Rahmanian, V. D.,1990, Siliciclastic sequence stratigraphy in well logs, cores, and outcrops: American Association of Petroleum Geologists Methods in Exploration Series, No. 7, 55p.

Figure Captions

Figure 1. Map of the Ferron Sandstone outcrops in east central Utah (stippled pattern). Also shown are the approximate locations of the pinchouts of the #4 and #5 marine sandstones from Ryer (1981a) and the locations of the measured stratigraphic sections.

Figure 2. Stratigraphic sections from Ryer (1981b) oriented approximately normal to the paleo-shoreline. See Figure 1 for locations of sections.

Figure 3. DVA plot and dip and azimuth histograms of bedding orientations measured in the #4 marine sandstone in the Miller Canyon, Muddy Creek and Dry Wash areas. Statistical parameters are listed on the dip histogram: n is the number of observations, gamma is the median, m is the unbiased efficient estimate of the mean, V2 is the unbiased efficient estimate of the variance, and v is the standard deviation.

Figure 4. Azimuth and dip versus depth plots of the #4 marine sandstone in the Dry Wash area.

Figure 5. Interpreted cross section and DVA plot for a fluvial channel in the Miller Canyon area.

Figure 6. DVA plot and dip and azimuth histograms of orientation measurements form the Miller Canyon and Muddy Creek area for bedding from the channels above the #4 marine sandstone. See the caption of Figure 3 for an explanation of the statistical parameters calculated for the dip angles.

Figure 7. DVA and dip and azimuth histograms of orientation measurements for the #5 marine sandstone. The data is from Muddy Creek and Dry Wash, and an explanation of the statistics can be found in Figure 1.

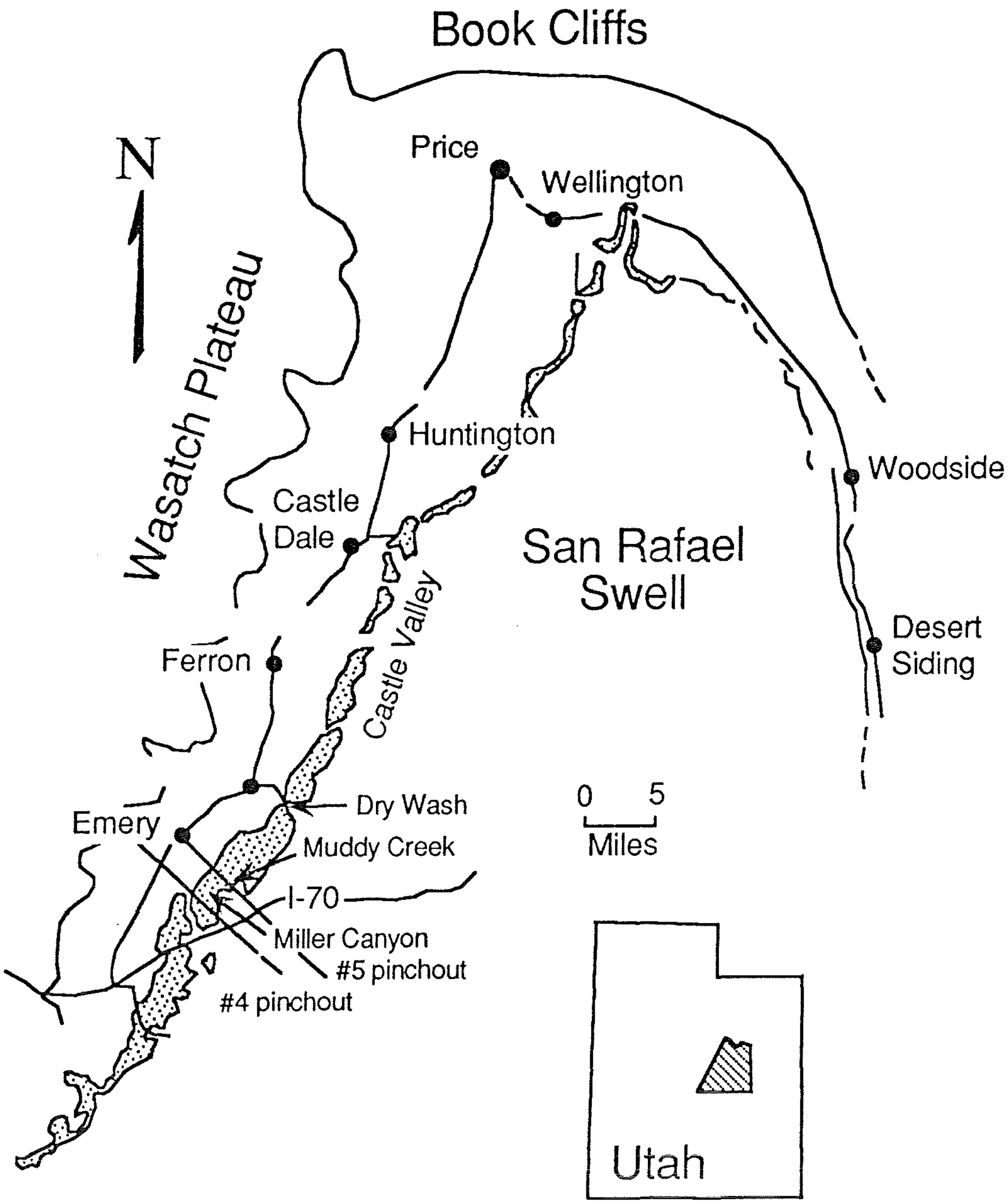
Book Cliffs
N
Wasatch Plateau
Price
Wellington
Huntington
Woodside
Castle Dale
San Rafael Swell
Castle Valley
Desert Siding
Ferron
Dry Wash
0 5 Miles
Emery
Muddy Creek
I-70
Miller Canyon
#5 pinchout
#4 pinchout
Utah

Fig. 1

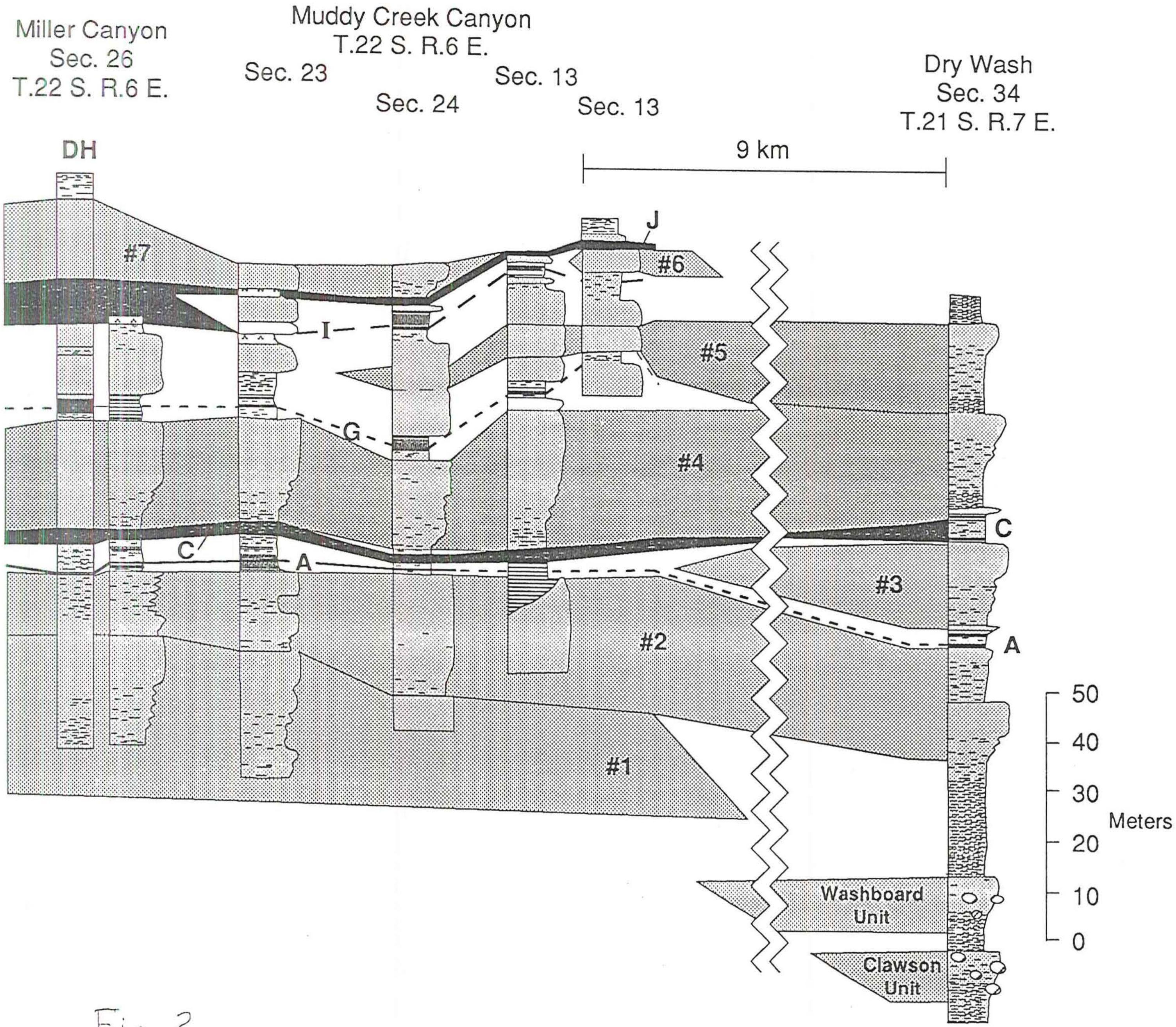
Miller Canyon
Sec. 26
T.22 S. R.6 E.
Muddy Creek Canyon
T.22 S. R.6 E.
Sec. 23
Sec. 24
Sec. 13
Sec. 13
Dry Wash
Sec. 34
T.21 S. R.7 E.
DH
9 km
J
#7
#6
I
#5
G
#4
C
C
A
#3
#2
A
#1
50
40
30
20
10
0
Meters
Washboard Unit
Clawson Unit

Fig. 2

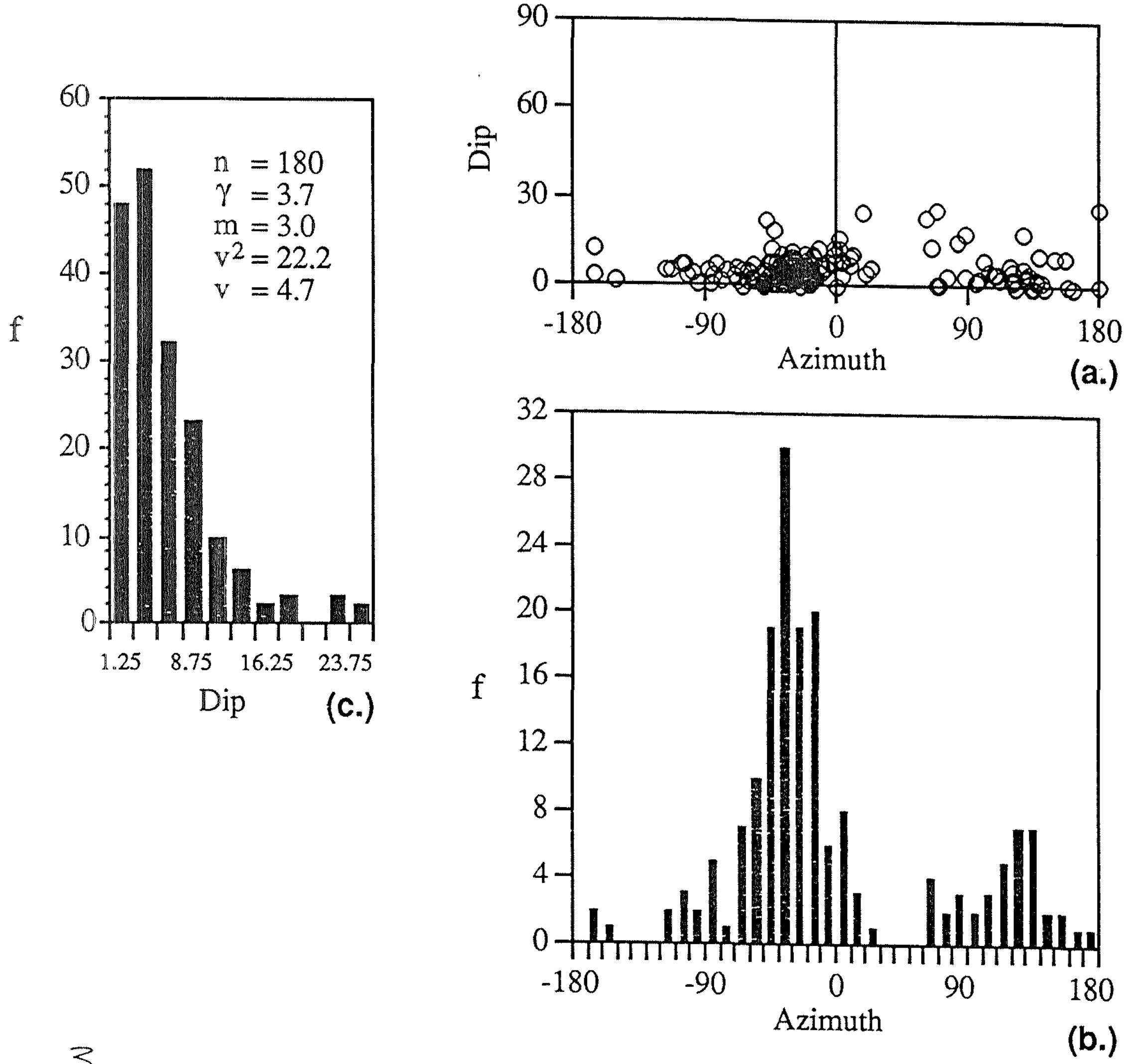
60
50
40
30
20
10
0
f
n = 180
γ = 3.7
m = 3.0
v2 = 22.2
v = 4.7
1.25
8.75
16.25
23.75
Dip
(c.)
90
60
30
0
Dip
-180
-90
0
90
180
Azimuth
(a.)
32
28
24
20
16
12
8
4
0
f
-180
-90
0
90
180
Azimuth
(b.)

Fig. 3

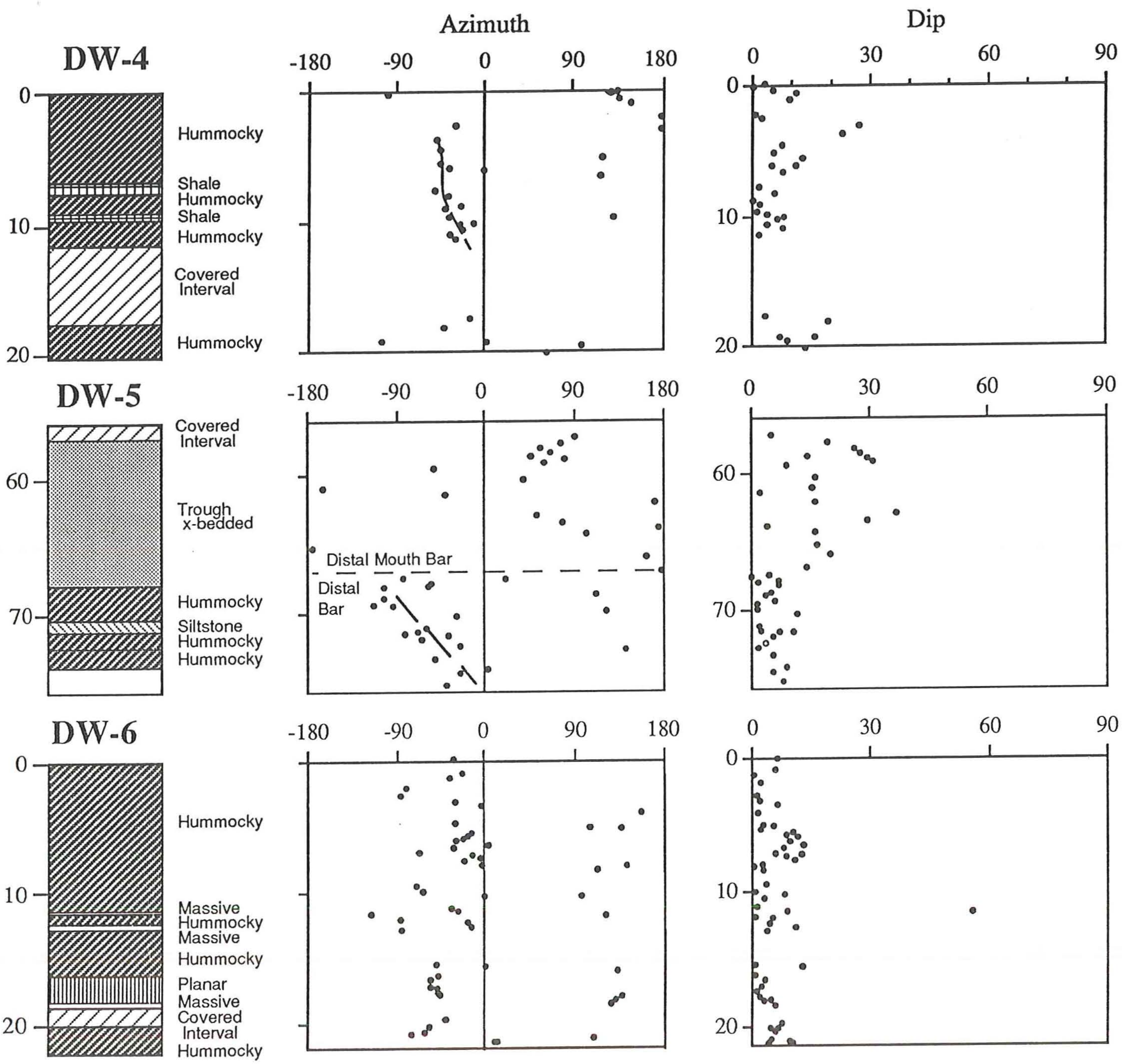
Azimuth
Dip
DW-4
-180
-90
0
90
180
0
30
60
90
0
10
20
Hummocky
Shale
Hummocky
Shale
Hummocky
Covered Interval
Hummocky
DW-5
60
70
Covered Interval
Trough x-bedded
Hummocky
Siltstone
Hummocky
Hummocky
Distal Mouth Bar
Distal Bar
DW-6
Hummocky
Massive
Hummocky
Massive
Hummocky
Planar
Massive
Covered Interval
Hummocky

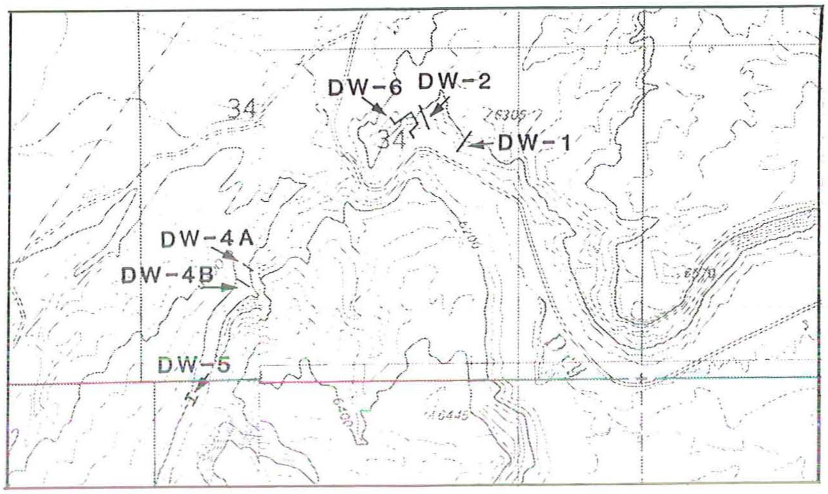
DW-6
DW-2
DW-1
34
34
DW-4A
DW-4B
DW-5

Fig. 4

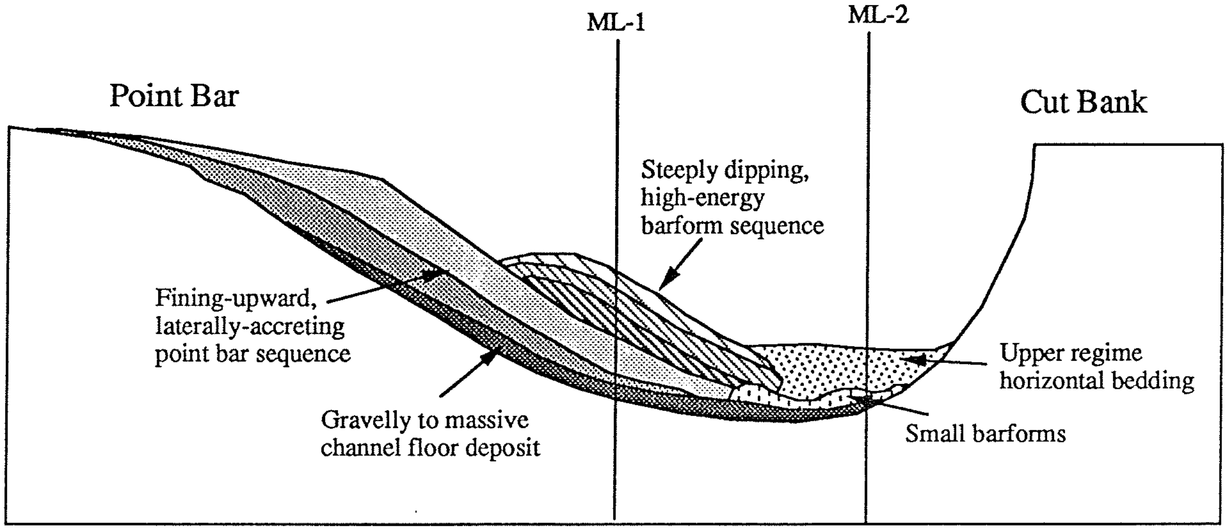
ML-1
ML-2
Point Bar
Cut Bank
Steeply dipping, high-energy barform sequence
Fining-upward, laterally-accreting point bar sequence
Upper regime horizontal bedding
Gravelly to massive channel floor deposit
Small barforms

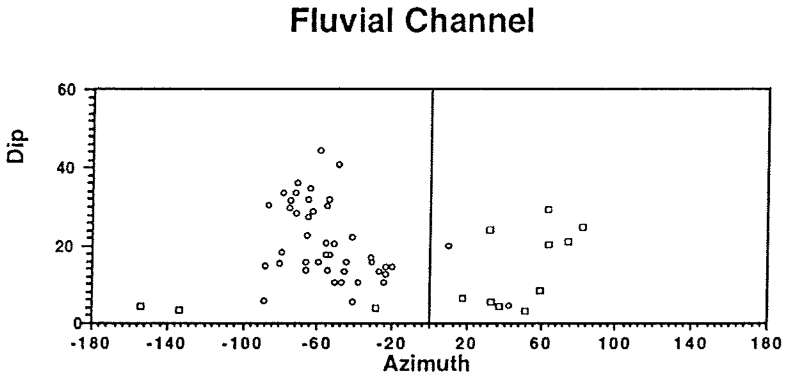
Fluvial Channel
Dip
60
40
20
0
-180
-140
-100
-60
-20
20
60
100
140
180
Azimuth

Fig. 5

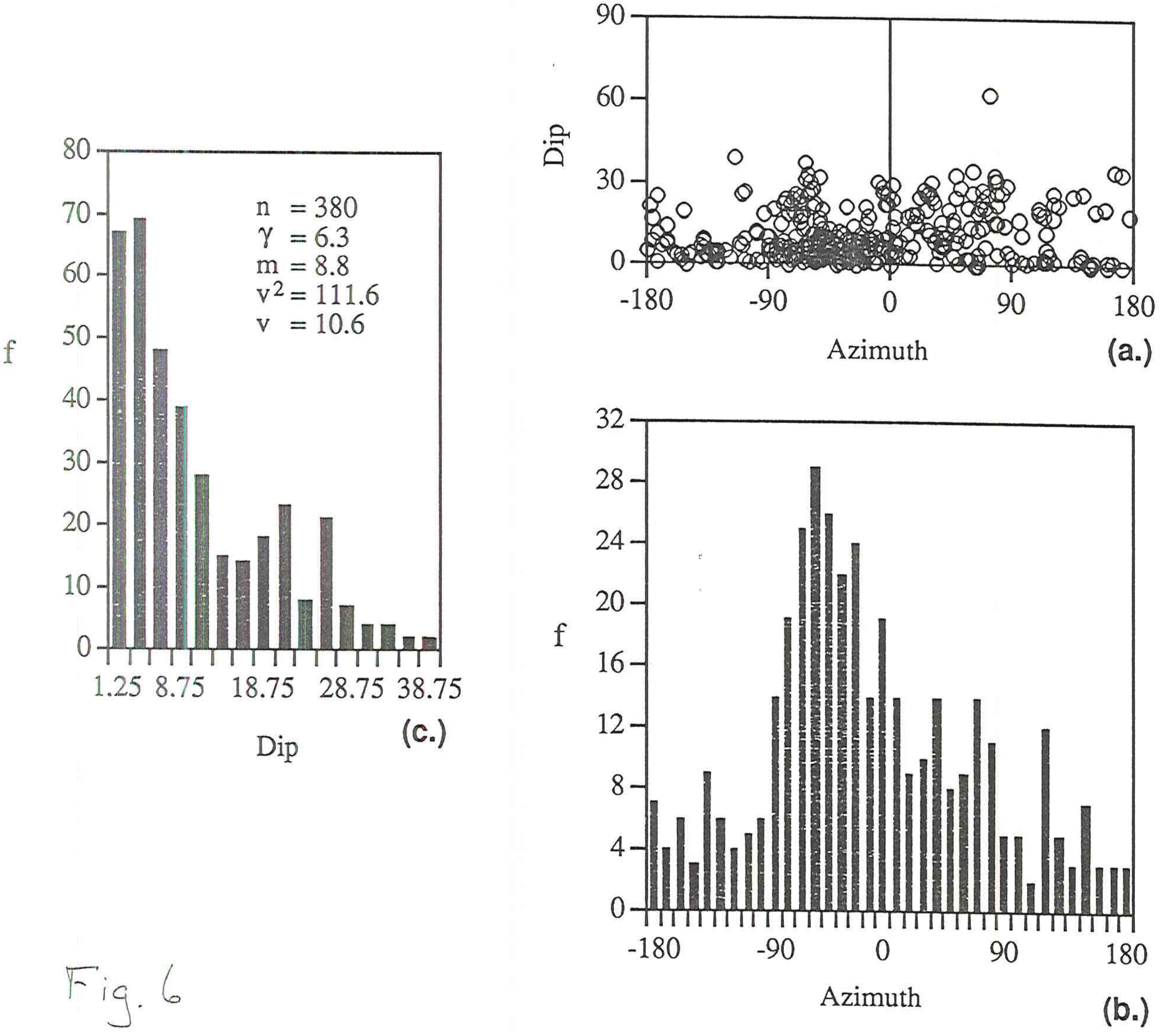
80
70
60
50
40
30
20
10
0
f
n = 380
γ = 6.3
m = 8.8
v^2 = 111.6
v = 10.6
1.25
8.75
18.75
28.75
38.75
Dip
(c.)
90
60
30
0
Dip
-180
-90
0
90
180
Azimuth
(a.)
32
28
24
20
16
12
8
4
0
f
-180
-90
0
90
180
Azimuth
(b.)

Fig. 6

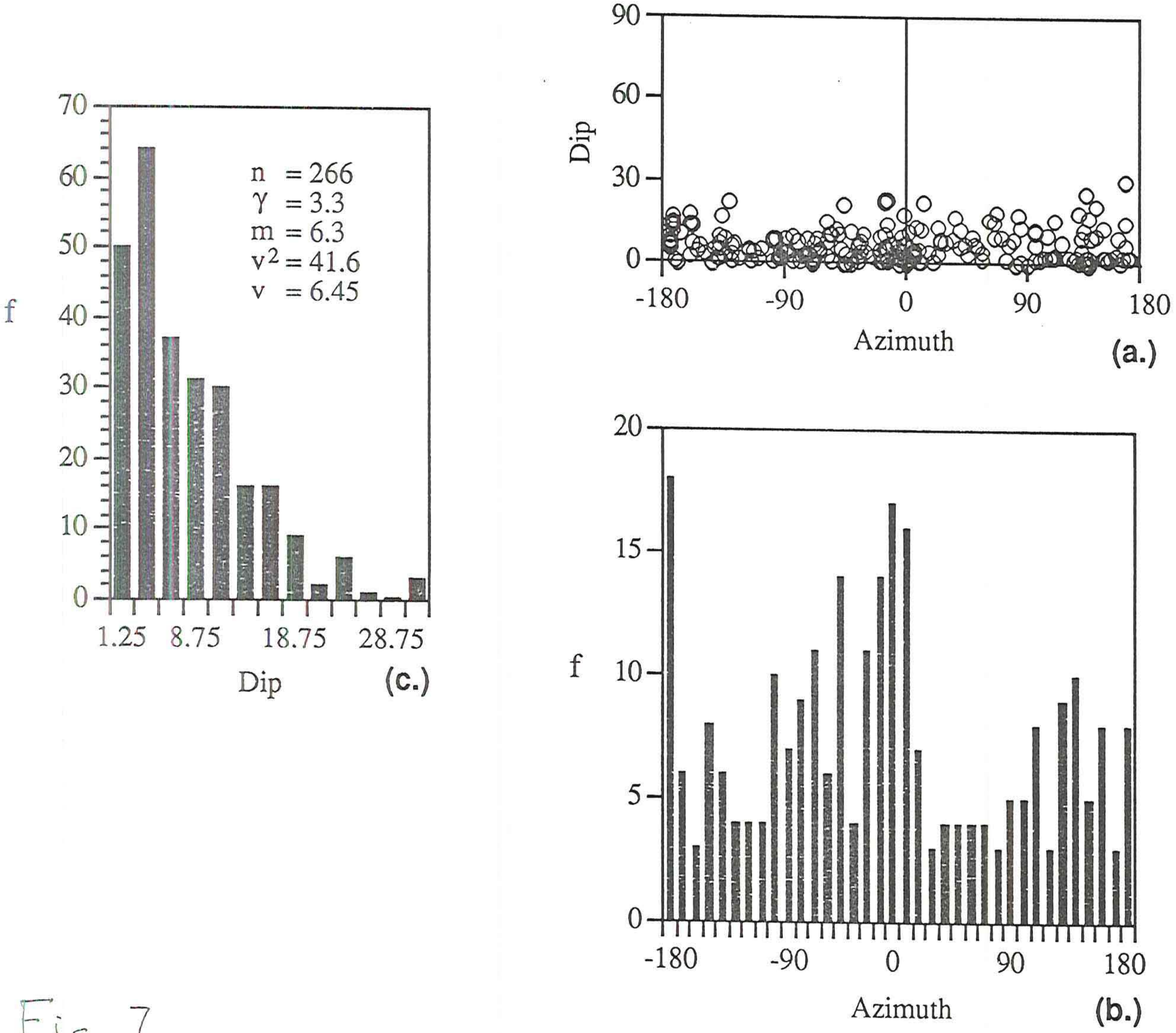
70
60
50
40
30
20
10
0
f
n = 266
γ = 3.3
m = 6.3
v² = 41.6
v = 6.45
1.25
8.75
18.75
28.75
Dip
(c.)
90
60
30
0
Dip
-180
-90
0
90
180
Azimuth
(a.)
20
15
10
5
0
f
-180
-90
0
90
180
Azimuth
(b.)

Fig. 7